Eleventh International Conference on CFD in the Minerals and Process Industries
CSIRO, Melbourne, Australia
7-9 December 2015

NUMERICAL MODELLING OF THE VELOCITY FIELD OF A PLANE JET FLOW AT MODERATE JET EXIT REYNOLDS NUMBERS

Ruth MOSSAD[1*] and Ravinesh C DEO[2]

[1] School of Mechanical and Electrical Engineering, University of Southern Queensland, QLD 4500, AUSTRALIA
[2] School of Agricultural, Computational and Environmental Sciences, University of Southern Queensland, QLD 4300, AUSTRALIA
*Corresponding author, E-mail address: ruth.mossad@usq.edu.au

ABSTRACT

A numerical prediction of the mean velocity distribution of a plane air jet issuing into the quiescent environment is conducted using the Standard *k-ε*, Realizable, k-ω and SST turbulent models. Different size meshes of approximately 8000, 1,760,000, and 5,000,000 grid points were used to guarantee the independence of the simulated flow from the mesh size factor. Various jet flow cases with Reynolds number based on the bulk mean velocity and the size of the inlet of 1500, 3000, 4400, 7100 and 10000 were modelled using the ANSYS-Fluent CFD software. A comparison of the simulated results with previous experimental measurements conducted using a hot wire anemometer showed relatively better agreement of the simulated velocity field with the experimental data when the Standard k-ε model was used, however the SST was tested only for the case of Reynolds number 1500 and it performed the best.

NOMENCLATURE

- h nozzle inlet size
- p pressure
- Re_h Reynolds number
- r^* nozzle profile-contraction factor, = r/h
- U_b bulk mean velocity
- U_c centreline velocity in x-direction
- $\overline{u}$ average velocity
- u' velocity fluctuation due to turbulence.
- V entrainment velocity
- W velocity along the z-plane, nominally zero
- w width along the span wise direction z
- ρ density
- ν kinematic viscosity of air
- μ dynamic viscosity
- τ *Stress tensor*
- x, y axial (streamwise) and lateral (y) directions

INTRODUCTION

A turbulent plane jet has been the subject of research since the pioneering work of Schlichting (1933). Several investigations focussed on the effects of initial conditions on jet flow behaviours (e.g. (Deo, 2005; Deo et al., 2004; Deo et al., 2007a, 2008; Deo et al., 2013; Everitt and Robins, 1978; Lemieux and Oosthuizen, 1985; Namer and Ötügen, 1988)). A great deal of attention on plane jet was mainly because of its flow statistics, described by mean, turbulent and higher order velocity or scalar statistics are represented as statistically two-dimensional fields. The two dimensionality of a plane jet is valuable for greater understanding and application of other jets in engineering areas such as the control of turbulent transport processes, understanding the mixing fields among the others (Stanley et al., 2002). A plane jet is treated as a prototypical flow to aid in understanding of fluid behaviour in propulsion, combustion, ventilation, air conditioning and environmental systems. The simplified statistics also offer advantages in turbulence research or numerical modelling, model validation and investigating eddy structures in moving fluids (Antonia et al., 1983). Henceforth, this article is devoted to furthering our understanding of the effect of Reynolds number on a plane jet using an experimental and a CFD modeling platform.

In experimental or modelling investigations, a plane jet is produced using a rectangular slot with dimensions ($w \times h$) and aspect ratio, $AR = w/h$, with $w >> h$, and w and h measured along the spanwise (z) and lateral (y) directions (Deo, 2005). A set of sidewalls attached to either end of the primary jet are used to restrict fluid entrainment in the spanwise (z) direction, so that the velocity, $W(x, y)$ along the z-plane is nominally zero. The self-sustaining jet is approximated to originate from a concentrated source of momentum and is typically analysed for the case where it issues into a quiescent (stagnant) or co-flowing environment. The main freestream velocity, $U(x, y)$ decays in the streamwise (x) direction that is also accompanied by a spreading in the y-direction proportional to the entrainment velocity, $V(x, y)$.

For a smoothly contoured nozzle, the time-averaged mean jet flow exhibits a potential core region immediately downstream of the exit up to an axial distance of $4 < x/h < 6$, in which $U(x, y)$ is uniform where the mean centreline velocity, $U_c(x, 0)$ approximately equals the bulk mean velocity, U_b. Within the interaction zone ($6 < x/h < 20$), the large-scale eddy structures interact with the ambient flow to transport gross momentum flux along the x-direction (Deo, 2005; Deo et al., 2004; Deo et al., 2007a, 2008; Deo et al., 2013). In the far field, the jet is self-preserving where statistical properties like spreading and velocity decaying rates, turbulence intensity, etc become invariant. Despite voluminous research on basic statistical parameters, much lesser number of studies has compared experimental and modelling results.

In this study, we aim to investigate the flow dynamics of a plane jet at various jet-exit Reynolds numbers (Re_h) given by

$$\mathrm{Re}_h = U_b h / \upsilon \quad (1)$$

U_b = area-averaged bulk mean velocity, υ = kinematic viscosity of fluid and h = characteristic length scale of the nozzle, taken as the smallest dimension of the nozzle, i.e. the "height" when the jet issues horizontally. The importance of Re_h using experimental investigations has been demonstrated in prior studies using a range of Re_h-values, although lesser number of investigations has used simulations at different values of Re_h. For example, the work of Lemieux and Oosthuizen (1985) tested Re_h values between $700 \leq Re_h \leq 4{,}200$, Suresh et al., (2008) tested Re_h between $250 \leq Re_h \leq 6{,}250$, Deo et al., (2008; 2013) used Re_h between $1{,}500 \leq Re_h \leq 10{,}000$ and Mi et al., (2009) used Re_h between 4,582–57,735. These investigations used experimental data to demonstrate the differences in flow structures relative to the disparities in Re_h values. A significant dependence of the exit and the downstream flow on Re_h demonstrated, despite all exit velocity profiles closely approximating a "top-hat" shape. The effect of Re_h on both the mean and turbulent fields was substantial for $Re_h \leq 10{,}000$ but this dependence becomes weaker with increasing Re_h, consistent with earlier work of Dimotakis (1983) for round jets. The length of the jet's potential core, initial primary-vortex shedding frequency, and far-field rates of decay and spread all depended on Reh.

Relative to the volume of experimental data available, there is significant paucity of model simulated data on plane jet flows, although modelling research is somewhat less expensive to perform with no requirement of logistics such as jet facilities other than a computational software, easiness for testing range of initial conditions without the need for constructing nozzles and industrial-scale trials can be performed with greater convenience. Specifically for plane jet flows, some simulated data using Reynolds averaged Navier–Stokes (RANS) is available, albeit at lower, and single Reynolds numbers. Numerical studies using RANS models were published by Heyerichs and Pollard (1996) at Re_h of 10,000, Hosseinalipour and Mujumdar (1997) also performed a similar study at a lower Reynolds number. Wang and Mujumdar (2007) compared five low Reynolds RANS models for two Re_h of 5200 and 10,400. Seyedein et al., (1995) performed another work using k-ε linear models for various Re_h The effect of boundary conditions on the heat transfer was studied by Shi et al., (2002) simulated jets at Re_h = 10,200 – 11,000 and Isman et al., (2008) using standard k-ε, LEVM, two NLEVMs and a differential Reynolds stress model over Re_h = 4 000–12 000. More recently, Jaramillo *et al*., (2012) performed a study on fluid flow and heat transfer in impinging plane jets for Re_h = 20,000.

The aforementioned investigations only measured the effect of Re_h on scalar field, particularly, heat transfer rates in plane jet flows. By contrast, lesser number of velocity field measurements were, for example by Klein et al., (2003) for $Re_h \leq 6000$ and Stanley and Sarkar (2002) for Re_h = 3000. Clearly, further modelling studies on velocity field of plane jets are warranted, so that the large and small-scale turbulent eddy structures that govern the mixing field can be investigated.

Although several comparisons have been performed in separate studies, to our best knowledge, no study has compared independently, the experimental and modelling results of a plane jet. Therefore, our study is motivated by a need to investigate the mean velocity field of a plane jet at a range of low to moderate Reynolds numbers, a regime where flow dynamics are expected to evolve differently with exit flow conditions (Deo et al., 2004; Deo et al., 2008; Deo et al., 2013; Mi et al., 2009).

EXPERIMENTAL AND MODELLING DETAILS

III. EXPERIMENTAL DESIGN

A. Plane jet facility

The experiment has been described in detail elsewhere (Deo, 2005; Deo et al., 2004; Deo et al., 2007a, 2008; Deo et al., 2013; Mi et al., 2009) so a summarised version is presented. All data were collected at the School of Mechanical Engineering, The University of Adelaide. Unheated air was supplied by an open circuit wind tunnel driven by a variable-speed, 14.5 kW aerofoil-type centrifugal fan. The flow was pre-conditioned by a diffuser, settling chamber, honeycomb and screens, feeding into a large, polynomial contraction. The exit of the contraction measured 720 mm × 340 mm, to which the plane jet nozzle was clamped securely. The plane jet nozzle was constructed from two perspex end plates, separated by slot height, h = 5.6 mm and width, w = 340 mm, figure 1. The inward edges were radially contoured with r = 12 mm. Consequently, the design ensured a sufficiently large aspect ratio, $AR = w/h = 60$ to produce statistically two-dimensional jet far into the self-preserving region (13) and the nozzle profile-contraction factor, $r^* = r/h \approx 2.14$ was necessary to produce mean exit velocity profile resembling the Blasius form (Deo et al.,

(a)

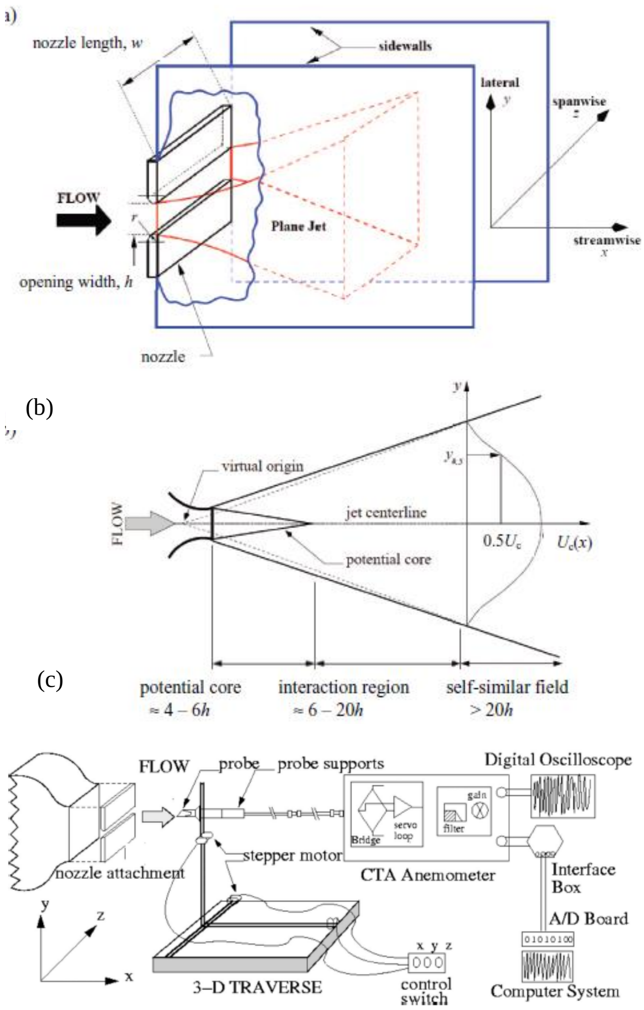

Figure 1: A schematic view of jet measurement facility.

B. Hot wire anemometry

A constant temperature anemometer (CTA) employing single hot wire probes was employed. A 3-dimensional traverse gear enabled measuring instruments to be traversed laterally (across the jet) and axially (direction of mean flow). The mean static pressure was measured with a Pitot static tube to calibrate the sensor. The streamwise component of instantaneous velocity, $U(x)$ was measured on the centreline over the region $0 \le x/h \le 160$, while the lateral component, $U(x, y)$ was measured at selected x/h across all isothermal jets for different values of Re_h.

A PC-30F data system operating at 200 kHz attached to a computer. After monitoring real-time raw signals on a Tektronix Oscilloscope, all data were visualized in WaveView 2.0 (DOS based data interface) for preliminary inspection. The input range of A/D board was ± 5.0 V, so an appropriate offset was applied to the sampled voltage to rectify the signal to remain within ± 3.0 V. This avoided clipping important tails of higher order moments of the fluctuating velocity signal (34). A cut-off frequency, f_c = 9.2 kHz was used to sample data at a Nyquist frequency of 18.4 kHz for 22.4 seconds to collect approximately 40 000 data points per measurement location. Based on the hot-wire calibrations and scatter in analysed data, estimated uncertainties in mean quantities were ~4.0% and those on the centre-plane were ~0.8%.

III. CFD MODELLING

The governing equations namely conservation of mass and momentum, in differential form for incompressible, steady, isothermal, three-dimensional, turbulent flow are given below:

$$\nabla \cdot \left(\rho \bar{\mathbf{u}}\right) = 0 \tag{2}$$

$$\nabla \cdot \left(\rho \bar{\mathbf{u}} \bar{\mathbf{u}}\right) = -\nabla p + \nabla . \mu \nabla \bar{\mathbf{u}} + \nabla \left(-\rho u' u'\right) \tag{3}$$

In these equations, $\bar{u}$ is the average velocity vector which has the component u, v and w, in the x, y and z directions, p is the average static pressure, and ρ is the density. Equation (2) is the time-averaged Navier-Stokes equation for turbulent flow in which $\nabla . \left(-\rho u' u'\right)$ is the Reynolds stresses, which depend on the turbulence model chosen. The governing equations are non-linear partial differential equations for which a closed form solution is not possible. The computational fluid dynamics software "ANSYS-Fluent", which uses a control volume-based finite difference method, was chosen to solve these equations, due to its good capability, and user-friendliness.

Four turbulent models were used in this work to examine which one predicts the flow more closely to the measured values. These turbulent models are the k-ε realizable (Shih et al., 1994), k-ε RNG (Choudhury, 1993; Yakhot and Orszag, 1986), the standard k-ε model (Speziale et al., 1991), the standard k-ω and the shear stress transport k-ω model SST.

The k-ε model is a semi-empirical model based on model transport equations for turbulent kinetic energy k and its dissipation rate ε. In fluent there are the standard, the realizable and the RNG k-ε models. The last two are improved version of the standard k-ε model which suits fully turbulent flow problems.

In regard to the k-ε realizable, it contains an alternative formulation for the turbulent viscosity and a modified transport equation for the dissipation rate ε which has been derived from an exact equation for the transport of the mean-square vorticity fluctuation (Shih et al., 1994) This turbulence model provides superior performance for flows involving rotation, boundary layers under strong adverse pressure gradients, separation, and recirculation. In regards to standard k-ω and the STT models, according to Menter et al. (2003) both has a similar form of transport equations for k and ω. However the SST has gradual change from the standard k-ω model in the inner region of the boundary layer to a high-Reynolds number version of the k-ε model in the outer part of the boundary layer and a modified turbulent viscosity formulation to account for the transport effects of the principal turbulent shear stress.

The non-equilibrium wall function was chosen with the realizable turbulent model which uses a two-layer based approach to include the pressure-gradient effects. The wall-neighbouring cells are assumed to consist of a viscous sublayer and a fully turbulent layer. The two layer approach is chosen to compute the budget turbulence kinetic energy in the wall-neighbouring cells using the Lauder and Spalding's log-law for mean velocity that is sensitized to pressure gradient effect, details can be found in Kim and Choudhury (1995). The first order upwind discretization was chosen for turbulent kinetic energy and turbulence dissipation rate to guarantee stability of the solution while the second order upwind discretization was used for the momentum and the PRESTO discretization (PREssure STaggering Option) was chosen for the pressure since it is more appropriate for flow with swirl and the SIMPLE method (Semi-Implicit Method for Pressure- Linked Equations) algorithm, was chosen for the pressure velocity coupling.

Only half of the domain was modelled by choosing a horizontal symmetry surface in the middle of jet inlet. Other boundary conditions were velocity at the inlet, and atmospheric pressure at outlet, non-slip condition on the walls surrounding the domain.

RESULTS

Comparison of the velocity along the centreline of the jet for the case of Reynolds number 1500 for the different hexahedral mesh sizes of 8000, 1,760,000 & 5,000,000 nodes using the standard k-ε model with the experimental results are given in Figure 2.

A comparison of the effect of mesh size on the centreline velocity is shown. It is evident that in the very near field, within the core of the plane jet ($0 \le d \le 0.1$) m, the experimental mean velocity profile collapses very well with the CFD model using the fine mesh. This region coincides with the potential core of the jet that usually contains pure jet fluid. However, from $0.1 \le d \le 0.7$, the experimental data is closer to the smallest and the medium mesh. While for $d > 0.7$ all mesh size prediction coincide with the experimental values. The exact cause of this discrepancy is not known yet, but will require further investigations to verify the cause of this.

Comparison of the experimental results of the velocity along the centreline of the jet for the cases of Reynolds number 1500, 3000, 4400, 7100, 10000 with the CFD model for the fine mesh using the standard *k-ε* and the realizable turbulent models are given in figures 3-7. Figure 3 compares the four turbulence model used for the case with Reynold number 1500.

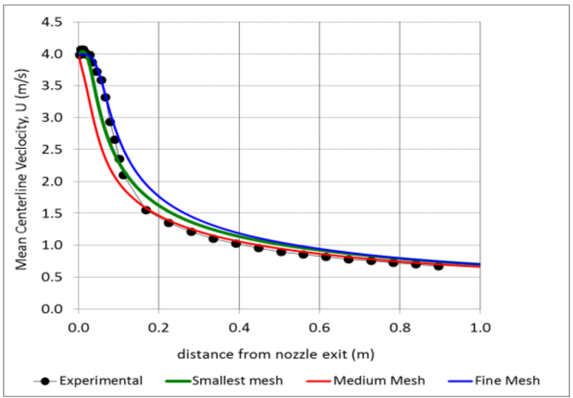

Figure 2: Comparison for the mean velocity along the jet centreline using *k-ε* model; for the case with Re_h = 1500.

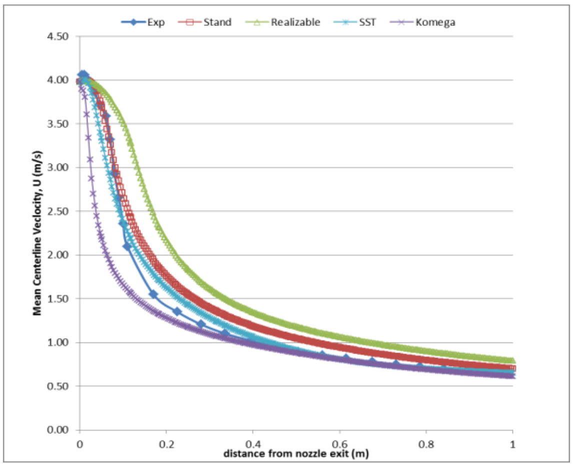

Figure 3: Re_h = 1500

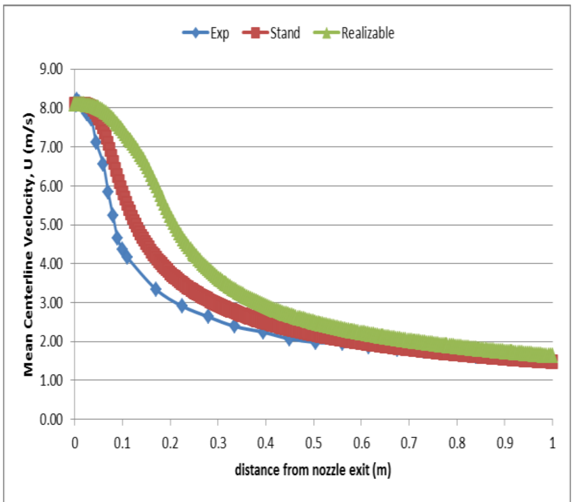

Figure 4: Re_h = 3000

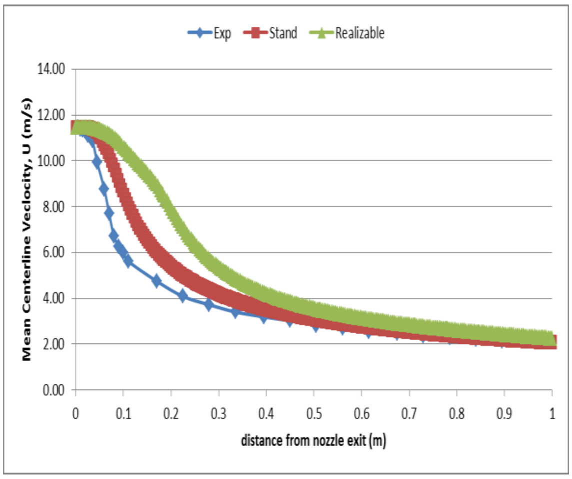

Figure 5: Reynolds number = 4400

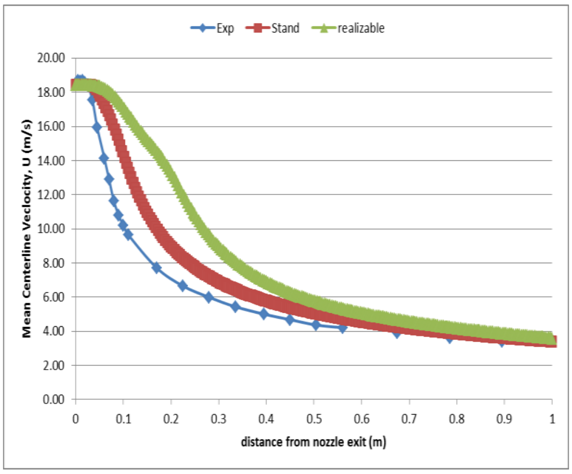

Figure 6: Re_h = 7100

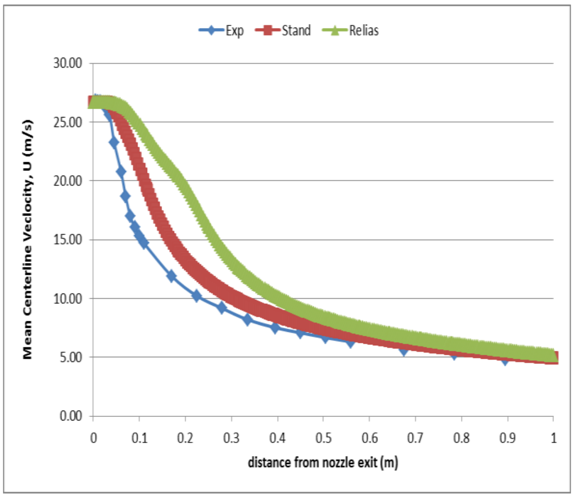

Figure 7: Re_h = 10000

In these figures one can see clearly that the standard *k-ε* model closely for all Reynolds number cases predicts the velocity distribution along the centreline when compared with the experimental results than the realizable turbulence model. However for the case with Reynolds number 1500, in which the four turbulence models were compared with the experimental results, it shows that the SST turbulent model performed the best.

The lateral profile of the mean velocity at x/h = 50 and 100 for the case of Re_h = 1500 are shown in Figure 8. It is noticeable that the simulated profiles have good agreement with the experimental profile for both locations.

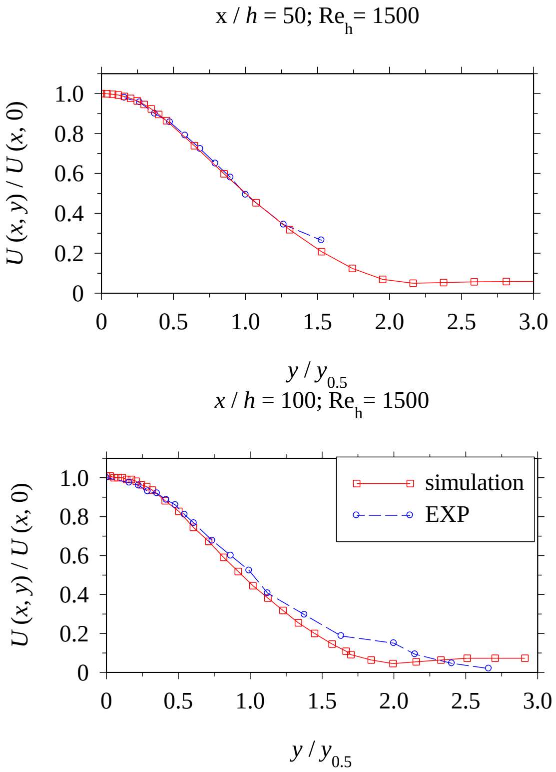

Figure 8: The lateral (y-direction) profile (x / h = 50 and 100) of the mean velocity $U(x, y)$ across the jet normalised by mean centreline velocity $U(x, 0)$ on ordinate axis and the jet half width $y_{0.5}$ on abscissa.

CONCLUSION

The comparison of the numerical model results for most Reynold numbers investigated with the experimental results showed that standard k-ε turbulent model is more appropriate to predict this type of flow than the realizable turbulent. However when the SST turbulence model was used for the case with Reynold number1500, it performed even better. The realizable turbulent model is known to provide superior performance for flows involving rotation, boundary layers under strong adverse pressure gradients, separation, and recirculation, which is not the case for a jet flowing in a motionless surrounding. Using the SST model with the rest of Reynold numbers and other turbulent models which are becoming available will be investigated in future research to find the most suitable model for this particular problem with which the difference between the model and the experimental results is minimized.

REFERENCES

ANTONIA, R., BROWNE, L., RAJAGOPALAN, S., CHAMBERS, A., (1983), "On the organized motion of a turbulent plane jet", *Journal of fluid mechanics*, **134**. 49-66.

CHOUDHURY, D., (1993), "*Introduction to the renormalization group method and turbulence modeling"*. Fluent Incorporated.

DEO, R., MI, J., NATHAN, G., (2004), "An investigation of the influence of nozzle aspect ratio on the velocity field of turbulent plane jet". *15th Australian fluid mechanic conference*.

DEO, R., C. (2005), "Experimental investigations of the influence of Reynolds number and boundary conditions on a plane air jet, PhD Thesis". *School of Mechanical Engineering*, The University of Adelaide, South Australia.

DEO, R.C., MI, J., NATHAN, G.J., (2007a), "The influence of nozzle aspect ratio on plane jets", *Experimental thermal and fluid science*, **31**. 825-838.

DEO, R.C., MI, J., NATHAN, G.J., (2007b), "The influence of nozzle-exit geometric profile on statistical properties of a turbulent plane jet", *Experimental Thermal and Fluid Science*, **32**. 545-559.

DEO, R.C., MI, J., NATHAN, G.J., (2008), "The influence of Reynolds number on a plane jet", *Physics of Fluids*, **20**, p. 075108.

DEO, R.C., NATHAN, G.J., MI, J., (2013), "Similarity analysis of the momentum field of a subsonic, plane air jet with varying jet-exit and local Reynolds numbers", *Physics of Fluids*, **25**, p. 015115.

DIMOTAKIS, P.E., MIAKE-LYE, R.C., PAPANTONIOU, D.A., (1983), "Structure and dynamics of round turbulent jets", *Physics of Fluids*, **26**. 3185-3192.

EVERITT, K., ROBINS, A., (1978), "The development and structure of turbulent plane jets", *Journal of Fluid Mechanics*, **88**. 563-568.

HEYERICHS, K., POLLARD, A., (1996), "Heat transfer in separated and impinging turbulent flows", *International Journal of Heat and Mass Transfer*, **39**. 2385-2400.

HOSSEINALIPOUR, S., MUJUMDAR, A., (1997), "Flow and thermal characteristics of steady two dimensional confined laminar opposing jets: Part I. Equal jets", *International Communications in Heat and Mass Transfer*, **24**. 27-38.

ISMAN, M., PULAT, E., ETEMOGLU, A., CAN, M., (2008), "Numerical investigation of turbulent impinging jet cooling of a constant heat flux surface", *Numerical Heat Transfer, Part A: Applications*, **53**. 1109-1132.

JARAMILLO, J., TRIAS, F., GOROBETS, A., PÉREZ-SEGARRA, C., OLIVA, A., (2012), "DNS and RANS modelling of a turbulent plane impinging jet", *International Journal of Heat and Mass Transfer*, **55**. 789-801.

KIM, S.-E., CHOUDHURY, D., (1995), "A near-wall treatment using wall functions sensitized to pressure gradient", *Separated and complex flows- 1995*. 273-280.

KLEIN, M., SADIKI, A., JANICKA, J., (2003), "Investigation of the influence of the Reynolds number on a plane jet using direct numerical simulation", *International Journal of Heat and Fluid Flow*, **24**. 785-794.

LEMIEUX, G., OOSTHUIZEN, P., (1985), "Experimental study of the behavior of plane turbulent jets at low Reynolds numbers", *AIAA journal*, **23**. 1845-1846.

MENTER, F.R., KUNTZ, M., LANGTRY, R. (2003), "Ten years of experience with the SST turbulence model". in: K. Hanjalic, Y.N., M. Tummers (Ed.), *Turbulence, Heat Mass Transfer*, Begell House. 625-632.

MI, J., FENG, B.-P., C, D.R., (2009), "Effect of exit Reynolds number on self-preservation of a plane jet".

NAMER, I., ÖTÜGEN, M., (1988), "Velocity measurements in a plane turbulent air jet at moderate Reynolds numbers", *Experiments in Fluids*, **6**. 387-399.

SCHLICHTING, H., (1933), "Laminare strahlausbreitung", *ZAMM-Journal of Applied Mathematics and Mechanics/Zeitschrift für Angewandte Mathematik und Mechanik*, **13**. 260-263.

SEYEDEIN, S., HASAN, M., MUJUMDAR, A., (1995), "Turbulent flow and heat transfer from confined multiple impinging slot jets", *Numerical Heat Transfer, Part A: Applications*, **27**. 35-51.

SHI, Y., RAY, M., MUJUMDAR, A., (2002), "Computational study of impingement heat transfer under a turbulent slot jet", *Industrial & Engineering Chemistry Research*, **41**. 4643-4651.

SHIH, T.-H., LIOU, W., SHABBIR, A., YANG, Z., ZHU, J., (1994), "A new k-epsilon eddy viscosity model for high Reynolds number turbulent flows: Model development and validation".

SPEZIALE, C.G., SARKAR, S., GATSKI, T.B., (1991), "Modelling the pressure–strain correlation of turbulence: an invariant dynamical systems approach", *Journal of Fluid Mechanics*, **227**. 245-272.

STANLEY, S., SARKAR, S., MELLADO, J., (2002), "A study of the flow-field evolution and mixing in a planar turbulent jet using direct numerical simulation", *Journal of Fluid Mechanics*, **450**. 377-407.

SURESH, P., SRINIVASAN, K., SUNDARARAJAN, T., DAS, S.K., (2008), "Reynolds number dependence of plane jet development in the transitional regime", *Physics of Fluids*, **20**, p. 044105.

WANG, X.-Q., MUJUMDAR, A.S., (2007), "Heat transfer characteristics of nanofluids: a review", *International journal of thermal sciences*, **46**. 1-19.

YAKHOT, V., ORSZAG, S.A., (1986), "Renormalization group analysis of turbulence. I. Basic theory", *Journal of scientific computing*, **1**. 3-51.

